

Lehmann-Symanzik-Zimmermann Reduction Approach to Multi-Photon Scattering in Coupled-Resonator Arrays

T. Shi and C. P. Sun

*Institute of Theoretical Physics,
Chinese Academy of Sciences, Beijing, 100190, China*

We present a quantum field theoretical approach based on the Lehmann-Symanzik-Zimmermann reduction for the multi-photon scattering process in a nano-architecture consisting of the coupled-resonator arrays (CRA), which are also coupled to some artificial atoms as a controlling quantum node. By making use of this approach, we find the bound states of single photon for an elementary unit, the T-type CRA, and explicitly obtain its multi-photon scattering S-matrix in various situations. We also use this method to calculate the multi-photon S-matrices for the more complex quantum network constructed with main T-type CRA's, such as a H-type CRA waveguide.

PACS numbers: 03.65.Nk, 42.50.-p, 11.55.-m, 72.10.Fk

I. INTRODUCTION

In order to realize all-optical quantum devices^{1,2}, it is very crucial to explore the physical mechanism for the single photon generation, transport and one shot detection *et al.*. Thus, we need a comprehensive understanding of the fundamental processes of coherent photonic scattering in the solid state based confined systems, such as the photonic crystal with artificial band gaps. Essentially, by coupling the system with an extra two-level system (TLS) to form a hybrid system, for controllably transport of photons the basic element is a quantum node or quantum switch³. It was abstracted as the so-called photon transistor most recently^{1,4}. For quantum information processing, such quantum node can coherently control the quantum state transfer in some quantum network⁵⁻⁷. Actually, to manipulate the coherent transport of photons, the quantum node is tunable so that it can behave either as a perfect mirror totally reflecting photons, or as an ideal transparent medium allowing photons to pass throughly. Theoretically, the quantum node for single-photon in all-optical architectures was extensively studied in one dimensional waveguide by making use of the standard scattering approaches^{2,8-13}.

The photonic quantum node is usually modelled as a localized TLS¹⁴, which can be implemented as an artificial atom, coupled to the photons transported in the coupled-resonator arrays (CRA)¹⁵. The atomic parameters, e.g., the energy level spacing, are tunable to control the propagation of photons. Recently, based on this theoretical model and its generalizations, the photon transport in the CRA systems has been studied for different purposes^{4,8,9,19}. Here, we would like to point out two remarkable issues: (a) if only one photon allowed to transport in the CRA with the artificial atom prepared at its ground state, the hybrid system can be described by a simple model with a single state coupled to a continuum, which is referred to the Anderson-Fano-Lee model¹⁶⁻¹⁸ with single excitation; (b) the CRA can be regarded as

the waveguide with nonlinear dispersion relation. It can be linearized in the high frequency regime in which photon momentum $k \sim \pm\pi/2a$ with lattice spacing a , to approximate the linear dispersion relation for the conventional waveguide.

In the recent study⁴, the single photon transmission and reflection coefficients were calculated for the incident photon with any energy in the T-type structure (a quantum node coupled to a CRA, see Fig. 1), which demonstrate the novel lineshapes beyond the Breit-Wigner²⁰ and the Fano lineshapes¹⁶. This kind of investigation was carried out only for the case with single photon. Also, there are only quite a few researches on the two photon case, for which we mention an elegant theoretical approach for two photon scattering^{8,9} based on the Bethe-ansatz²¹⁻²⁷. Moreover, we have to say that it sounds very difficult to prepare the system only with one photon or two photons exactly, thus these previous studies need to be improved for multi-photon processes oriented by practical application.

Actually, the study for multi-photon transport is very important to realize a practical all-optical devices. However, these subtle approaches for single and two photon cases mentioned above^{4,8,9,19}, such as the discrete coordinate scattering theory and the Bethe-ansatz technique with fixed scatterers, are not feasibly generalized for the realistic multi-photon processes, even for two-photon or three-photon processes. Therefore, our present systematic approach based on quantum field theory is significant since it is obviously feasible and intrinsically natural for the generalization to multi-photon scattering processes.

In this paper, we utilize the Lehmann-Symanzik-Zimmermann (LSZ) reduction²⁸ in quantum field theory to investigate the multi-photon transport in the complex CRA with some two-level scatterers. This method has been used to study the single electron inelastic scattering in Anderson model and Kondo model^{29,30}. Here, we deal with the multi-photon scattering problem by studying the out-state of the scattered photons for an arbitrary

state of incident photons. In a middle stages, we calculate the multi-photon scattering matrix (S -matrix) in details. With the diagrammatic analysis, we find that the basic element of the S -matrix is a connected transfer matrix (T -matrix), which can be obtained from the well-known LSZ reduction formula about the photonic Green's function. From the explicitly achieved expressions of photonic out-states, we analysis in details quantum statistical characters of photon transmission in the situation with many photons. We find that, in the tight binding CRA of T-type, there exist the single photon bound states. As a test, two photon transport in the T-type waveguide is re-considered, and our obtained results accord with the recent works^{8,9} using the Bethe-ansatz, which verifies the results based on the LSZ reduction approach are valid. As the development, the three photon scattering is studied, and the outgoing states of the three photon are given by this approach. Our present investigation mainly based on these results, can be regarded as a substantial development for its particular emphasis on the multi-photon scattering.

In practice, the T-type photonic element we mentioned above is the basic block to constitute a complex quantum network coherently transferring photons in a controllable fashion. A slightly complicated illustration of such architecture is the CRA waveguide of H-type. In this paper, we also study two photon scattering processes in the H-type in details.

The paper is organized as follows: in Sec. II and III, we model our hybrid system for multi-photon transport and present the scattering matrix based on the LSZ reduction approach; in Sec. IV, we show that there exist the single photon bound states in the tight binding T-type CRA; in Sec. V, we study the multi-photon transport in the T-type waveguide; in Sec. VI, we discuss the two photon transport in the H-type waveguide; in Sec. VII, the results are summarized with some remarks.

II. SCATTERING MODEL FOR THE HYBRID SYSTEM

A. Model setup

In this subsection, we model the T-type CRA by the two-level atom coupled to photons inside CRA illustrated in Fig. 1. The model Hamiltonian reads

$$H_T = \Omega |e\rangle\langle e| + \sum_i [\omega_0 a_i^\dagger a_i - J(a_i^\dagger a_{i+1} + \text{H.c.})] + V \sum_i \delta_{i0} (a_i^\dagger \sigma^- + \text{h.c.}), \quad (1)$$

where the operator $\sigma^- = |g\rangle\langle e|$ denotes the flip from the atomic ground state $|g\rangle$ to the excited state $|e\rangle$ with the energy level spacing Ω . Here, J is the hopping constant characterizing the inter-cavity coupling in the tight-binding approximation; $a_i (a_i^\dagger)$ is the

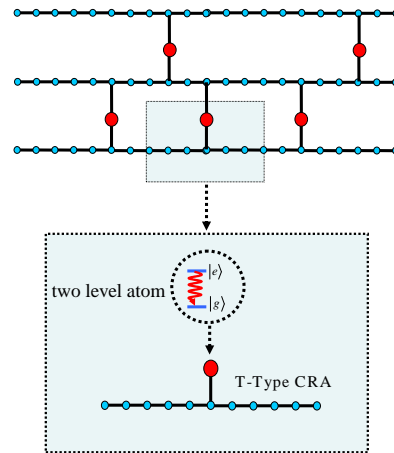


FIG. 1: (Color online) The schematic for the complex CRA: The T-type structure with CRA coupled to impurity (maybe a two-level scatterer) is the basic element to construct the more complicated architecture of quantum network. The red circles denote the two level impurity, while the blue dots denote the photonic coupled resonators.

annihilation (creation) operator for the photonic single mode with eigen-frequency ω_0 in the i -th cavity; V is the hybridization constant of the localized atom-photon in the 0-th site of CRA.

In the momentum space (k -space), the Hamiltonian (1) is re-expressed as

$$H_T = \Omega |e\rangle\langle e| + \sum_k \varepsilon_k a_k^\dagger a_k + \frac{V}{\sqrt{L}} \sum_k (a_k^\dagger \sigma^- + \text{H.c.}), \quad (2)$$

with the photonic dispersion relation

$$\varepsilon_k = \omega_0 - 2J \cos k, \quad (3)$$

in CRA of length L . Here, we choose the cavity spacing $a = 1$. In the high energy limits $k \sim \pm\pi/2$ and $\omega_0 = \pi J$, the above dispersion relation is linearized as $\varepsilon_k \sim |k|$, which is the same as that in the conventional waveguide. Thus, we can use CRA to simulate the conventional waveguide in the high frequency limits. As the basic element of the complex quantum network as illustrated in Fig. 1, the two-level atom plays the role of the photon transistor to control the photon transmission.

It is obvious that, when confined within the single excitation subspace, our model is the same as the models by Anderson, Fano and Lee. This observation motivates us to consider how to use various approaches developed previously for the models by Anderson, Fano and Lee, to deal with the coherent processes of our system, especially with multi-photons. To this end, we will compare our model (2) with the Anderson, Fano and Lee model as follows.

B. Relation to Anderson model

By neglecting the Coulomb interaction, the Anderson model is the same as the Fano model, so we discuss the similarities and differences between the model (2) and Anderson model. The corresponding Hamiltonian reads

$$H_A = \sum_{k,\sigma} \varepsilon_k c_{k\sigma}^\dagger c_{k\sigma} + \varepsilon_d f_\sigma^\dagger f_\sigma + H_V + H_U, \quad (4)$$

where $c_{k\sigma}$ ($c_{k\sigma}^\dagger$) is the annihilation (creation) operator of the conductive electron with dispersion relation ε_k and spin σ . f_σ (f_σ^\dagger) is the annihilation (creation) operator of the impurity f -electron with energy ε_d and spin σ . The Coulomb repulsive interaction of the impurity f -electrons is described by the Hubbard term $H_U = U f_\uparrow^\dagger f_\uparrow f_\downarrow^\dagger f_\downarrow$. The hybridization of a conductive electron with the localized f -electron is depicted by the mixing term

$$H_V = V \sum_{k,\sigma} (c_{k\sigma}^\dagger f_\sigma + \text{H.c.}). \quad (5)$$

Anderson even used this model (4) to investigate the localized magnetic state in the metal. By comparing the Hamiltonian (4) with the Hamiltonian (2), we find that the atom and the photon in the model (2) can be considered as the impurity f -electron and the conductive electron in the Anderson model, respectively. But there still exist some differences between the two models. First, the Hilbert space of the atom in the model (2) is spanned by two basis states, $|e\rangle$ and $|g\rangle$, but the Hilbert space of the impurity f -electron is spanned by four basis states, $|0\rangle$, $f_\uparrow^\dagger |0\rangle$, $f_\downarrow^\dagger |0\rangle$ and $f_\uparrow^\dagger f_\downarrow^\dagger |0\rangle$. Secondly, in the Anderson model the conductive electrons are fermions, while in the model (2) photons are bosons. Thirdly, there is no Hubbard term H_U in the model (2), while in the Anderson model if there is only one f -electron the Coulomb interaction vanishes, i.e., the Hubbard interaction H_U does not play any role. In conclusion, the two models are equivalent only in the single excitation case, i.e., one conductive electron with no f -electron or one impurity f -electron with no conductive electron in the Anderson model, and one photon with the atom prepared at the ground state or no photon with the atom prepared at the excited state in the model (2). Otherwise, in the multi-excitation case, the two models (2) and (4) are obviously not equivalent.

C. Relation to Lee model

The Lee model¹⁸ with the Hamiltonian

$$H_L = m_V \psi_V^\dagger \psi_V + m_N \psi_N^\dagger \psi_N + \sum_k \omega_k A_k^\dagger A_k + g \sum_k \frac{1}{\sqrt{2\omega_k V}} (\psi_V^\dagger \psi_N A_k + \text{H.c.}), \quad (6)$$

describes a reaction process

$$V \rightleftharpoons N + A_k, \quad (7)$$

with two heavy fermions (V , N) of masses m_V and m_N . Here, the relativistic boson A_k with momentum k and rest mass μ possesses the dispersion relation $\omega_k = \sqrt{k^2 + \mu^2}$, and g is the three body coupling constant for the scattering of the three kinds of particles, V , N , and A . T. D. Lee used this exact solvable model to study the necessity of renormalization in quantum field theory even without the perturbation expansion.

By comparing Lee model with the model (2), we find that the heavy fermions V and N can be regarded as the excited state and ground state of the atom, respectively. And the relativistic boson A_k can be considered as the photon in the model (2). There also exist some differences between the Lee model and the model (2). Firstly, in Lee model, the renormalizations of the V -fermion mass m_V and coupling constant g should be taken into account, and the Hamiltonian (6) is non-Hermitian. Thus we should investigate the unitarity of the S -matrix carefully^{31,32}. Secondly, the Hilbert space of heavy fermion is spanned by four basis states, i.e., $|0\rangle$, $\psi_V^\dagger |0\rangle$, $\psi_N^\dagger |0\rangle$ and $\psi_V^\dagger \psi_N^\dagger |0\rangle$. We conclude that the two models (2) and (6) are equivalent only in the single excitation case, i.e., one relativistic boson A_k with one heavy fermion N or one heavy fermion V with no relativistic boson A_k in Lee model, and one photon with the atom prepared at the ground state or no photon with the atom prepared at the excited state in the model (2).

In fact, it is turn out that the multi-particle scattering problems (such as N - $\theta\theta$ scattering) in the Anderson and Lee models were both successfully studied by the LSZ reduction approach^{29,30,33,34}. In the following, we start with the model (2) to investigate the S -matrix of scattering photon in the hybrid CRA systems. For the further discussion, we first give a general formalism to study the multi-photon S -matrix in the complex CRA by the LSZ reduction formalism.

III. LEHMANN-SYMANZIK-ZIMMERMANN REDUCTION FOR PHOTON SCATTERING IN GENERAL

In this section, we first briefly summarize the main results of the LSZ reduction approach in quantum field theory, and then we use them to give a general formula for multi-photon S -matrix in the T-type CRA. For investigating the multi-photon scattering, in the first subsection, we first define the n -photon S -matrix and $2n$ -point photonic Green's function, which are explicitly described by the Feynman diagrams (Fig. 2), and utilized the functional integral to obtain the $2n$ -point photonic Green's function. In the second subsection, we use the LSZ reduction approach to obtain a general form of the n -photon S -matrix element by reducing the external legs (red curves in Fig. 2) of the Green's function.

A. Main results of the LSZ reduction approach

Because the LSZ reduction approach relates to the photonic Green's function and S -matrix, we need to give their definitions for discussing the LSZ reduction explicitly. The $2n$ -point photonic Green's function

$$G_{p_1, \dots, p_n; k_1, \dots, k_n}(t'_1, \dots, t'_n; t_1, \dots, t_n) = \langle \Theta | T a_{p_1}(t'_1) \dots a_{p_n}(t'_n) a_{k_1}^\dagger(t_1) \dots a_{k_n}^\dagger(t_n) | \Theta \rangle, \quad (8)$$

is defined by the time ordering product T of the photon creation (annihilation) operator a_k^\dagger (a_k) in the Heisenberg picture. Here, Θ denotes the ground state of the Hamiltonian H of the system.

The S -matrix element^{35,36}

$${}_{out} \langle f | i \rangle_{in} = {}_{in} \langle f | S | i \rangle_{in}. \quad (9)$$

of photons is defined through the overlap of incoming state $|i\rangle_{in}$ and outgoing scattering state $|f\rangle_{out}$, which are asymptotically free, and may contain multi-photon excitation, i.e., they are multi-photon states. In our case, the incoming state is

$$|i\rangle_{in} = a_{k_1}^\dagger \dots a_{k_n}^\dagger |0\rangle. \quad (10)$$

In the present case, the S -matrix is given by

$$S = T \exp[-i \int_{-\infty}^{+\infty} dt H_{int}(t)], \quad (11)$$

with the atom-photon hybridization Hamiltonian

$$H_{int} = V(a_0^\dagger \sigma^- + \text{H.c.}), \quad (12)$$

in the interaction picture.

Using the diagrammatic analysis, we find that the Feynman diagram of S -matrix element is constructed by summing up the contributions from all kinds of disconnected diagrams as shown in Fig. 2. Here, each of these disconnected diagram is made up of some connected diagrams which describe the T -matrix elements. As the special cases, we consider the diagrammatic construction for the single photon and the two photon S -matrix elements by the connected T -matrix elements below. For the single photon case, the S -matrix element

$$S_{p;k} = \delta_{kp} + iT_{p;k}, \quad (13)$$

is defined by the T -matrix element for single photon, where k and p are the momenta of the incoming and outgoing photons. In this case, there exist two kinds of disconnected diagrams (a) and (b) as shown in Fig. 3.

For the two photon case, the S -matrix element

$$S_{p_1 p_2; k_1 k_2} = S_{p_1 k_1} S_{p_2 k_2} + S_{p_2 k_1} S_{p_1 k_2} + iT_{p_1 p_2; k_1 k_2}, \quad (14)$$

is reduced by the T -matrix element of two photons, where k_r and p_r ($r = 1, 2$) are the momenta of the incoming and outgoing photons. In this case, there exist three kinds

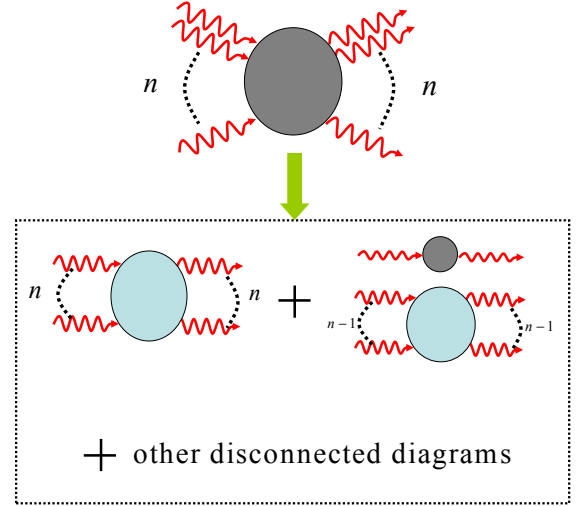


FIG. 2: (Color online) The Feynman diagrams for LSZ reduction: The red line denotes the free photon propagator. The gray shade circles denote the S -matrix elements and the blue shade circles denote the T -matrix elements. The Feynman diagram of S matrix element is constructed by all kinds of

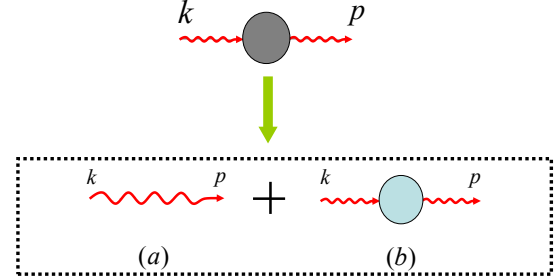


FIG. 3: (Color online) The diagrammatic constructions of the single photon S -matrix element: There exist two kinds of disconnected diagrams (a) and (b). The red line denotes the free photon propagator. The gray shade circles denote the S -matrix elements and the blue shade circles denote the single photon T -matrix elements.

of disconnected diagrams (a), (b) and (c) as shown in Fig. 4. Obviously, the multi-photon S -matrix is totally determined by the connected T -matrix, so we only need to find the photonic T -matrices.

Fortunately, the intrinsic relation

$$iT_{2n} = G_{2n} \prod_{r=1}^n [2\pi G_0^{-1}(k_r) G_0^{-1}(p_r)] \Big|_{os}, \quad (15)$$

between n -photon T -matrix element

$$T_{2n} = T_{p_1, \dots, p_n; k_1, \dots, k_n}, \quad (16)$$

and photonic Green's function

$$G_{2n} = G_{p_1, \dots, p_n; k_1, \dots, k_n}, \quad (17)$$

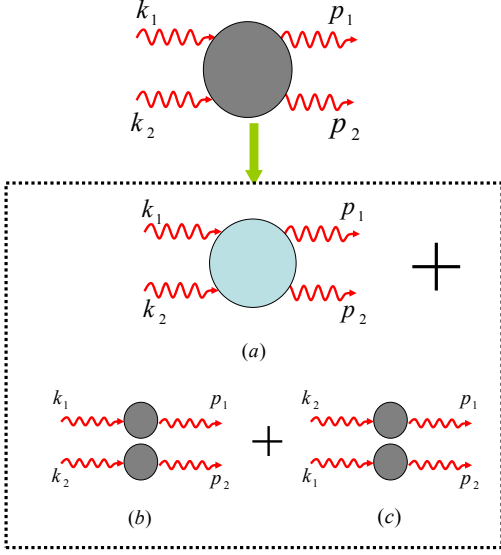


FIG. 4: (Color online) The diagrammatic constructions of the two photon S -matrix element: There exist three kinds of disconnected diagrams (a), (b) and (c). The red line denotes the free photon propagator. The gray shade circles denote the S -matrix elements and the blue shade circles denote the two photon T -matrix elements.

is given by the LSZ reduction formula, where

$$G_0(k_r) = \frac{i}{\omega_r - \varepsilon_{k_r} + i0^+}, \quad (18)$$

is the Green's function of free photon and $G_{p_1, \dots, p_n; k_1, \dots, k_n}$ is the Fourier transformation of Eq. (8). Here, the subscript os denotes the on shell limit $\omega \rightarrow \varepsilon_k$. Finally, the multi-photon S -matrix elements are determined by the photonic Green's functions entirely. In this paper, we use an elegant method, i.e., functional integrals, to establish the desired relation (15). This method has been used to solve many quantum impurity problem^{29,30} in the condensed matter physics. Here, we show how it works for the multi-photon transmission in this hybrid system.

B. General formula for S -matrix in the T-type CRA

We utilize the generating functional Z to represent the full time ordering Green's function as

$$G_{p_1, \dots, p_n; k_1, \dots, k_n} = \frac{(-1)^n \delta^{2n} \ln Z[\eta_k, \eta_k^*]}{\delta \eta_{p_1}^* \dots \delta \eta_{p_n}^* \delta \eta_{k_1} \dots \delta \eta_{k_n}} \Big|_{\eta_k = \eta_k^* = 0}, \quad (19)$$

where the generating functional

$$Z[\eta, \eta^*] = \int D[a_k a_k^\dagger] D[f_\sigma f_\sigma^\dagger] \delta(\sum_\sigma f_\sigma^\dagger f_\sigma - 1) \exp\{i[S + \int dt \sum_k (\eta_k^* a_k + \eta_k a_k^\dagger)]\}, \quad (20)$$

is defined by the action $S = \int dt L$ and the Lagrangian

$$L = i f_e^\dagger \partial_t f_e + i f_g^\dagger \partial_t f_g + i \sum_k a_k^\dagger \partial_t a_k - H_T. \quad (21)$$

In Eq. (20), we represent the two-level atom by the fermions f_σ as

$$\begin{aligned} |e\rangle \langle e| &= f_e^\dagger f_e, \\ |e\rangle \langle g| &= f_e^\dagger f_g, \end{aligned} \quad (22)$$

with the constraint

$$\sum_{\sigma=e,g} f_\sigma^\dagger f_\sigma = 1. \quad (23)$$

This constraint arises from the fact that the physical space of the atom spanned by $|e\rangle$ and $|g\rangle$ is two dimensions, while the physical space of the fermions spanned by $|0\rangle$, $f_e^\dagger |0\rangle$, $f_g^\dagger |0\rangle$ and $f_e^\dagger f_g^\dagger |0\rangle$ is four dimensions. By integrating the photon field and the fermionic fields f_σ in Eq. (20), the generating functional is obtained as

$$\begin{aligned} \ln Z[\eta, \eta^*] &= Tr \ln M[\xi, \xi^*] \\ &\quad - i \int d\omega dk \frac{|\eta_k(\omega)|^2}{\omega - \varepsilon_k + i0^+}, \end{aligned} \quad (24)$$

where the field variable is

$$\xi(\omega) = V \int \frac{dk}{2\pi} \frac{\eta_k(\omega)}{\omega - \varepsilon_k + i0^+}, \quad (25)$$

and the matrix

$$M[\xi, \xi^*] = \begin{pmatrix} [\omega - \Omega + \Sigma(\omega)] \delta_{\omega\omega'} & \xi(\omega - \omega') \\ \xi^\dagger(\omega' - \omega) & (\omega - i0^+) \delta_{\omega\omega'} \end{pmatrix}, \quad (26)$$

is defined by the self-energy

$$\Sigma(\omega) = Re\Sigma(\omega) + i \frac{\Gamma}{2} \rho(\omega), \quad (27)$$

of the atom and $\Gamma = V^2$. Here, the real part of the self-energy is determined by the principal-value integral as

$$Re\Sigma(\omega) = \int \frac{dk}{2\pi} P \frac{\Gamma}{\varepsilon_k - \omega}, \quad (28)$$

and the imaginary part is proportional to the density of state (DOS)

$$\rho(\omega) = \sum_i \frac{1}{|D_i(\omega)|}, \quad (29)$$

where $D_i(\omega) = \partial_k \varepsilon_k|_{k=z_i}$ and z_i is the real root of the equation $\varepsilon_{z_i} = \omega$. For the waveguide the self-energy $\Sigma(\omega)$ is a constant. For the CRA the self-energy depends on the frequency ω and we have used Markov approximation to obtain Eq. (24).

With the helps of Eqs. (15), (19) and (24), we can achieve the multi-photon S -matrix by considering the Green's function G_{2n} . In the following, we use the LSZ approach to study the multi-photon transport in the complex CRA.

IV. BOUND STATES OF THE SINGLE PHOTON TRANSPORT IN THE T-TYPE CRA

In this section, we consider the single photon transport in the T-type CRA. This problem has been considered in Ref.⁴, but the photon bound states have not been taken into account. There are two interesting physical phenomena about the photon bound states. (a) Firstly, in the hybrid system the single photon bound states depict the states that the single photon is almost localized in the cavity containing the two-level atom. In this sense, the photon bound states can be used as the quantum information storage of single photon. (b) Secondly, as the basic element of single photon transistor, the T-type CRA is usually coupled with other CRAs through the two-level atom. These CRAs can be regarded as the scattering channels. It is proved that¹⁹ the incident photon in another CRA, whose energy is resonance on the bound state energy in the T-type CRA, will be totally reflected. This phenomenon can be considered as the one-dimension photonic Feshbach resonance, which can be used to simulate the Feshbach resonance in the atomic and condensed matter physics. The above reasons motivate us to study the photon bound states in the T-type CRA by using the LSZ approach.

The T-type CRA is described by the Hamiltonian (2). Then Eqs. (15), (19) and (24) immediately give the single photon S -matrix element

$$S_{p;k} = (1 + r_k)\delta_{kp} + r_k\delta_{-kp}, \quad (30)$$

with the reflection amplitude

$$r_k = \frac{-i\Gamma}{2J \sin k (\varepsilon_k - \Omega) + i\Gamma}. \quad (31)$$

Here, we have utilized DOS $\rho(\omega) = 2/\sqrt{4J^2 - (\omega - \omega_0)^2}$ and $Re\Sigma(\omega) = 0$ for the scattered photon in the T-type CRA. The result (30) is the same as that obtained in Ref.⁴.

In the following, we study the single photon bound states in this system by considering the poles of S -matrix (see Fig. 5a). The poles of S -matrix are the roots of the equation

$$(E_b - \Omega) + i\frac{\Gamma}{2}\Sigma(E_b) = 0. \quad (32)$$

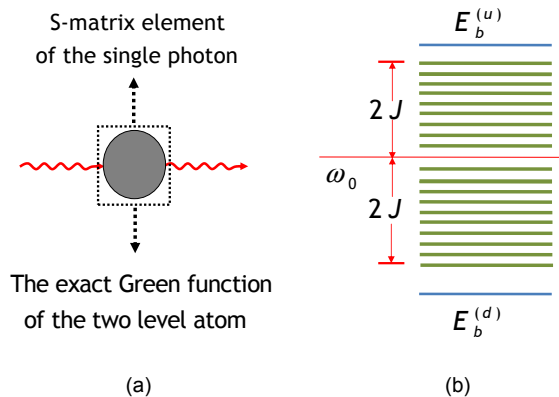


FIG. 5: (Color online) (a) The gray shade circle denotes the scattering matrix element of the single photon, and it is also the Green function of the two level atom. The poles of the atom Green function determine the energies of the bound states. (b) The band structure of T-type CRA is shown in the right panel.

Because the energies of bound states are not inside the photonic energy band of the CRA, i.e., $|E_b - \omega_0| > 2J$, the self-energy is

$$\Sigma(E_b) = -\frac{\Gamma \text{sign}(E_b - \omega_0)}{\sqrt{(E_b - \omega_0)^2 - 4J^2}}. \quad (33)$$

Then Eq. (32) becomes

$$E_b - \Omega - \frac{\Gamma \text{sign}(E_b - \omega_0)}{\sqrt{(E_b - \omega_0)^2 - 4J^2}} = 0. \quad (34)$$

The above equation possesses two solutions ($E_b^{(d)}$ and $E_b^{(u)}$) for E_b : one solution $E_b^{(d)}$ is below the bottom of energy band, the other solution $E_b^{(u)}$ is above the top of energy band. The structure of the energy spectrum is shown in Fig 5b. The two bound states are

$$|B_{\pm}\rangle = [\sum_i \psi_{\pm}(x_i) a_i^{\dagger} + \sigma^{\pm}] |0\rangle, \quad (35)$$

with the wave-functions¹⁹ in the spatial representation

$$\begin{aligned} \psi_{-}(x_i) &= \frac{(-)^{|x_i|} V}{\sqrt{(E_b^{(u)} - \omega_0)^2 - 4J^2}} e^{|x_i| \ln \kappa_{-}(E_b^{(u)})}, \text{ if } E_b = E_b^{(u)} \\ \psi_{+}(x_i) &= \frac{V}{\sqrt{(E_b^{(d)} - \omega_0)^2 - 4J^2}} e^{|x_i| \ln \kappa_{+}(E_b^{(d)})}, \text{ if } E_b = E_b^{(d)}, \end{aligned} \quad (36)$$

where

$$\kappa_{\pm}(E) = -\sqrt{\left(\frac{E - \omega_0}{2J}\right)^2 - 1} \pm \frac{\omega_0 - E}{2J}. \quad (37)$$

It is obviously that $\ln \kappa_{\pm}(E) < 0$ for the both cases $E = E_b^{(u)}$ and $E = E_b^{(d)}$; the wave functions exponentially decay as $|x|$ increases as shown in Eq. (36), which

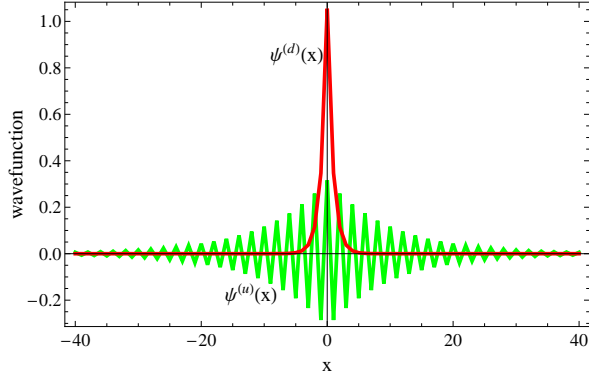


FIG. 6: (Color online) The wave-functions of two photonic bound state in the discrete coordinates. The norms of both wave-functions exponentially decay as $|x|$ increases.

insure that the photon is indeed localized to form the bound states. The wave-functions $\psi_{\pm}(x_i)$ are illustrated in Fig. 6.

By short summary for this section, we verify the existence of photon bound states in the T-type CRA by considering the poles of the S -matrix element. In the next section, using the T-type CRA to simulate the T-type waveguide, we study the multi-photon transport in the T-type waveguide.

V. SCATTERING MATRIX FOR PHOTONS IN THE T-TYPE WAVEGUIDE

In this section, we focus on the photon transport in the T-type waveguide. For the T-type waveguide, S -matrix element is firstly calculated out by the LSZ reduction. Secondly, by using the obtained S -matrix, we give the out-state for arbitrary incident state of photons. Finally, by analyzing the photon out-state in the spatial representation, we can obtain the quantum statistical properties of the scattered photons, such as the photon bunching and anti-bunching.

As shown in Sec. II, the waveguide is simulated by CRA in the limits $k \sim \pm\pi/2$ and $\omega_0 = \pi J$, in which the dispersion relation of the photon is $\varepsilon_k = v_g |k| = |k|$. Here, we let the group velocity $v_g = 1$ for convenient. Then the Hamiltonian

$$H_T = \Omega |e\rangle\langle e| + \sum_k |k| a_k^\dagger a_k + \frac{V}{\sqrt{L}} \sum_k (a_k^\dagger \sigma^- + \text{H.c.}), \quad (38)$$

describing the T-type waveguide becomes

$$H_T^{(w)} = H_T^e + H_T^o, \quad (39)$$

with two parts

$$H_T^o = \sum_{k>0} \varepsilon_k a_{k,o}^\dagger a_{k,o}, \quad (40)$$

and

$$H_T^e = \Omega |e\rangle\langle e| + \sum_{k>0} k a_{k,e}^\dagger a_{k,e} + \frac{\tilde{V}}{\sqrt{L}} \sum_{k>0} (a_{k,e}^\dagger \sigma^- + \text{H.c.}), \quad (41)$$

where the operators

$$a_{k,e} = \frac{1}{\sqrt{2}} (a_k + a_{-k}),$$

$$a_{k,o} = \frac{1}{\sqrt{2}} (a_k - a_{-k}), \quad (42)$$

describe annihilations of the e -photon and o -photon. Here, e -photon depicts the photon with even parity in the momentum space, i.e., $a_{-k,e} = a_{k,e}$, and o -photon depicts the photon with odd parity in the momentum space, i.e., $a_{-k,o} = -a_{k,o}$. In Eq. (41), the effective coupling constant is $\tilde{V} = \sqrt{2}V$. For the o -photon, the H_T^o is diagonalized in the bases $\{a_{k,o}^\dagger |0\rangle\}$, so we only need to find out the S -matrix for the scattered e -photon. In the following, we consider the S -matrix for the e -photon according to the approach.

A. Single photon scattering

For the single e -photon case, Eqs. (19) and (24) give the single photon Green's function

$$G(p; k) = [G_0(k) - \frac{i}{2\pi} \frac{\Gamma_T}{\omega_k - \alpha} G_0^2(k)] \delta_{pk}, \quad (43)$$

where $\alpha = \Omega - i\Gamma_T/2$ and $\Gamma_T = \tilde{V}^2$. Here, we used $Re\Sigma(\omega) = 0$ and $\rho(\omega) = 1$. Together with Eq. (15), Eq. (43) gives the single e -photon T -matrix

$$iT_{p;k} = \delta_{pk} \frac{-i\Gamma_T}{k - \alpha}. \quad (44)$$

Next, we achieve the single e -photon S -matrix element $S_{p;k} = t_k \delta_{pk}$ by considering Eq. (13), where the transmission coefficient is

$$t_k = \frac{k - \alpha^*}{k - \alpha}. \quad (45)$$

This result (45) accords with that of Refs.^{8,9} based on the Lippmann-Schwinger formalism.

B. Two photon scattering

For the two e -photon case, Eqs. (19) and (24) give the two e -photon Green's function as follows:

$$G_{p_1, p_2; k_1, k_2} = i \frac{2\Gamma_T^2}{(2\pi)^3} \frac{G_0(k_1)G_0(k_2)G_0(p_1)G_0(p_2)}{(\omega'_2 - \alpha)(\omega'_1 - \alpha)} \times \frac{(\omega_1 + \omega_2 - 2\alpha)\delta_{\omega_1 + \omega_2, \omega'_1 + \omega'_2}}{(\omega_1 - \alpha)(\omega_2 - \alpha)}. \quad (46)$$

By taking the photon frequency ω_i and ω'_i on shell, we obtain the T -matrix

$$iT_{p_1, p_2; k_1, k_2} = i \frac{\Gamma_T^2}{\pi} \frac{(k_1 + k_2 - 2\alpha)}{(p_2 - \alpha)(k_1 - \alpha)} \times \frac{\delta_{k_1 + k_2, p_1 + p_2}}{(p_1 - \alpha)(k_2 - \alpha)}. \quad (47)$$

From the above equation, the two e -photon S -matrix element

$$S_{p_1 p_2; k_1 k_2} = iT_{p_1 p_2; k_1, k_2} + t_{k_1} t_{k_2} (\delta_{p_1 k_1} \delta_{p_2 k_2} + \delta_{p_2 k_1} \delta_{p_1 k_2}). \quad (48)$$

follows Eq. (14) immediately. If two incident photons are prepared in the state $|k_1, k_2\rangle$, the wave function^{8,9}

$$\begin{aligned} \langle x_c, x | out \rangle &= \frac{1}{2} \sum_{p_1 p_2} S_{p_1 p_2; k_1 k_2} \langle x_c, x | p_1, p_2 \rangle \\ &= e^{iEx_c} \frac{1}{2\pi} [t_{k_1} t_{k_2} \cos(\Delta_k x) \\ &\quad - \frac{4\Gamma_T^2 e^{i(E-2\Omega+i\Gamma_T)|x|/2}}{4\Delta_k^2 - (E-2\Omega+i\Gamma_T)^2}], \quad (49) \end{aligned}$$

of two outgoing photons in the spatial representation is obtained in terms of the two e -photon center of mass coordinate $x_c = (x_1 + x_2)/2$ and two photon relative coordinate $x = x_1 - x_2$. Here, the total momentum (energy) is $E = k_1 + k_2$ and the relative momentum is $\Delta_k = (k_1 - k_2)/2$. When the photon momenta k_1 and k_2 both satisfy the resonance condition $k_1 = k_2 = \Omega$, the envelop wave-function (49) exponentially decays as the relative coordinate x increases. This reflects that the outgoing two photons attract with each other effectively and form a two photon bound state. If $E - 2\Omega$ is kept to zero, the wave-function at $x = 0$ decreases as $|\Delta_k|$ increases, which implies the photons repulse against each other effectively through interacting with the two-level atom. The above results about two photon scattering accord with the results reported in Refs.^{8,9}.

C. Three photon scattering

For the three photon case, Eqs. (15) and (19) give the connected T -matrix as

$$iT_{p_1 p_2 p_3; k_1 k_2 k_3} = i \frac{\Gamma_T^3}{3(2\pi)^2} \delta[\sum_i (k_i - p_i)] \sum_{a=1,2,3} F_{k_i, p_i}^{(a)}, \quad (50)$$

where the functions $F_{\omega_i, \omega'_i}^{(a)}$ are defined as

$$F_{\omega_i, \omega'_i}^{(1)} = \sum_{PQ} \frac{\prod_i \delta(\omega_i - k_{P_i})}{(\omega'_1 - \omega_1)(\omega'_3 - \omega_3)(\omega_1 - \alpha)} \frac{\prod_i \delta(\omega'_i - p_{Q_i})}{(\omega'_3 - \alpha)(\omega_1 + \omega_2 - \omega'_1 - \alpha)}, \quad (51)$$

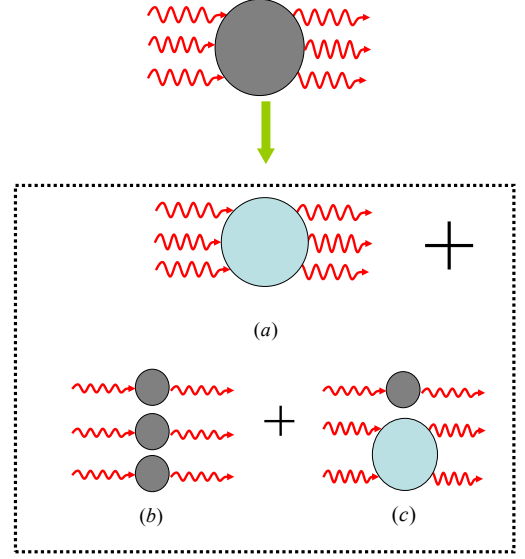


FIG. 7: (Color online) Feynman diagrams for three photon S matrix: There exist three kinds of disconnected diagrams (a), (b) and (c).

$$F_{\omega_i, \omega'_i}^{(2)} = \sum_{PQ} \frac{\prod_i \delta(\omega_i - k_{P_i})}{(\omega'_2 - \omega_2)(\omega'_3 - \omega_3)(\omega'_2 - \alpha)} \frac{\prod_i \delta(\omega'_i - p_{Q_i})}{(\omega_3 - \alpha)(\omega'_2 + \omega'_1 - \omega_2 - \alpha)}, \quad (52)$$

and

$$F_{\omega_i, \omega'_i}^{(3)} = \sum_{PQ} \frac{\prod_i \delta(\omega_i - k_{P_i})}{(\omega'_2 - \omega_2)(\omega'_1 - \omega_1)(\omega'_1 - \alpha)} \frac{\prod_i \delta(\omega'_i - p_{Q_i})}{(\omega_2 - \alpha)(\omega_2 + \omega_3 - \omega'_2 - \alpha)}. \quad (53)$$

Here, $P = (P_1, P_2, P_3)$ and $Q = (Q_1, Q_2, Q_3)$ are two different permutations of $(1, 2, 3)$, and $i = 1, 2, 3$. The three photon S -matrix element

$$\begin{aligned} S_{p_1, p_2, p_3; k_1, k_2, k_3} &= i \sum_{i,j=1,2,3} \sum_{\gamma, \delta \neq i} \sum_{\lambda, \beta \neq j} S_{p_j; k_i} T_{p_\lambda, p_\beta; k_\gamma, k_\delta} \\ &\quad + \sum_{PQ} \prod_{i=1,2,3} S_{p_{Q_i}; k_{P_i}} \\ &\quad + iT_{p_1, p_2, p_3; k_1, k_2, k_3}, \quad (54) \end{aligned}$$

is constructed by summing up the contributions from all disconnected Feynman diagrams as shown in Fig. 7. Here, $\gamma, \delta, \lambda, \beta \in \{1, 2, 3\}$. The similar discussions can be applicable to deal with the N -photon scattering process.

Next, we consider the physical meaning of S -matrix. To this end, we first analysis the T -matrices, which are $|T_2|^2 = |T_{p_1 p_2; k_1, k_2}|^2$ and $|T_3|^2 = |T_{p_1, p_2, p_3; k_1, k_2, k_3}|^2$. Here, $|T_2|^2$ describes the two-photon background fluorescence, which is explicitly discussed in Ref.^{8,9}, and $|T_3|^2$

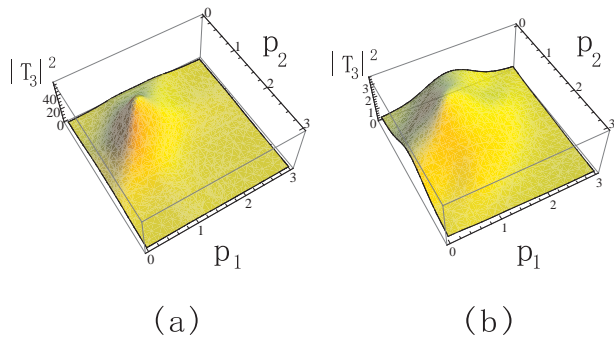


FIG. 8: (Color online) Three-photon background fluorescence for the total energy of incident photons $E = k_1 + k_2 + k_3 = 3$ and $\Gamma_T = 1$, where the energy level spacing Ω is taken as units: (a) the three photon are both on resonance with the atom, i.e., $k_1 = k_2 = k_3 = \Omega$; (b) the energies of the three photons are $k_1 = 0.5$, $k_2 = 0.3$, and $k_3 = 2.2$, respectively.

depicts the three-photon background fluorescence, which is shown in Fig. 8. It is shown that when the three photons are all on resonance with the atom, the three-photon background fluorescence describing $|T_3|^2$ is enhanced largely.

The out-going state of three photons

$$|out\rangle = \sum_{p_1 \leq p_2 \leq p_3} S_{p_1, p_2, p_3; k_1, k_2, k_3} |p_1, p_2, p_3\rangle, \quad (55)$$

is determined by the three photon S -matrix, and its spatial representation the wave-function reads as

$$\begin{aligned} & \langle x_1, x_2, x_3 | out \rangle \\ &= \sum_{p_1 p_2 p_3} \frac{S_{p_1, p_2, p_3; k_1, k_2, k_3}}{6(2\pi)^{3/2}} e^{i(p_1 x_1 + p_2 x_2 + p_3 x_3)}. \end{aligned} \quad (56)$$

The contour maps of the probability distributions $|\langle x_1, x_2, x_3 | out \rangle|^2$ are numerically shown in Fig. 9. It is illustrated in Fig. 9a that when the three photon are all on resonance with the atom, the scattered photons prefer the two photon bound state rather than the three photon bound state. That is, if two photons form the bound state, it is difficult to form three photon bound state, namely, the two bounded photons repulse another one effectively. When the three photon are not on resonance, the probability distribution $|\langle x_1, x_2, x_3 | out \rangle|^2$ is shown in Fig. 9b. It is illustrated in Fig. 9b that it is also difficult to realize the three photon bound state. If the position of one photon is given, such as $x_3 = 0$, other two photons do not always attract or repulse each other, but attract each other at some points and repulse each other at other points, which are determined by the distance between the two photon and another photon localized at $x_3 = 0$. It follows the above discussion that, in the conceptual setup of the photon transistor, the two-level atom controls the coherent transport behaviors of single photon, such as the transmission and reflection. In the

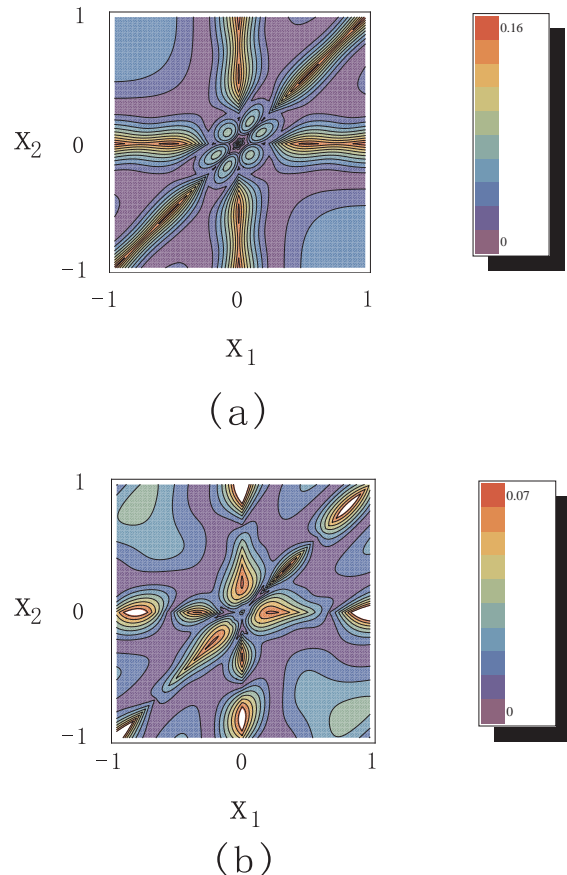


FIG. 9: (Color online) The probability distribution of three photon with one photon at origin, where the total energy of incident photons $E = k_1 + k_2 + k_3 = 3$, the energy spacing Ω is taken as units, and $\Gamma_T = 1$: (a) the three photon are both on resonance with the atom, i.e., $k_1 = k_2 = k_3 = \Omega$; (b) the energies of the three photons are $k_1 = 0.5$, $k_2 = 1.5$, and $k_3 = 1$, respectively.

multi-photon transport, the atom can induce the effective interaction of photons. We can control the effective interaction by adjusting the energy level spacing of the atom. Therefore, the coherent manipulations of TLS can result in a transitions from the repulsive case to attraction of effective photon interactions.

In addition, we point that the recent references^{8,9} obtained the same results for two photons transport, but our works are different from them: (1) Refs.^{8,9} only give the two photon eigenstates by Bethe-ansatz method, but we find a general method^{37,38}, i.e., the scattering Bethe ansatz technique (see Appendix), to derive the multi-photon eigenstates; (2) though we can obtain the multi-photon eigenstates by the subtle scattering Bethe-ansatz method, we still need a lot of complicated calculations to achieve the S -matrix by using the Lippmann-Schwinger scattering theory. However, the LSZ approach can be generalized to study the multi-photon scattering in the

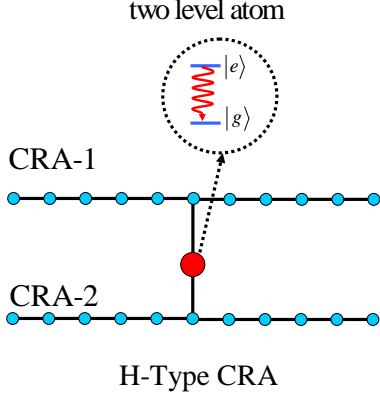


FIG. 10: (Color online) The schematic for the H-type CRA is shown in this figure. The red circle denotes the two level atom. The blue dots denote the coupled resonators.

waveguide, such as the three photon transport in the waveguide; (3) Except these, the LSZ approach is also used to deal with the multi-photon scattering in the more complex CRA, such as the H-type CRA. In the next section, by using the H-type CRA to simulate the H-type waveguide, we investigate the multi-photon transport in the H-type waveguide.

VI. TWO PHOTON SCATTERING PROCESS IN THE H-TYPE WAVEGUIDE

In this section, we study the two photon scattering process in the H-type waveguide. The conventional H-type waveguide is simulated by the H-type CRA (Fig. 10) in the high energy limits. The model Hamiltonian

$$H_H = \Omega |e\rangle \langle e| + \sum_{i,s=1,2} \delta_{i0} (V_s a_{i,s}^\dagger \sigma^- + h.c.) \quad (57)$$

$$+ \sum_{i,s=1,2} [\omega_0^{(s)} a_{i,s}^\dagger a_{i,s} - J_s (a_{i,s}^\dagger a_{i+1,s} + h.c.)],$$

of the H-type CRA is defined by the hopping constant J_s and the creation operator $a_{i,s}^\dagger$ of the i -th single mode cavity with frequency $\omega_0^{(s)}$ in the CRA- s , where V_s is the hybridization constant of localized atom-photon in the 0-th site of the CRA- s . Here, s denotes the CRA-1 or the CRA-2 as shown in Fig. 10. In the k -space, the Hamiltonian (57) becomes

$$H_H = \Omega |e\rangle \langle e| + \sum_{k,s=1,2} \varepsilon_k^{(s)} a_{k,s}^\dagger a_{k,s}$$

$$+ \frac{1}{\sqrt{L}} \sum_{k,s=1,2} (V_s a_{k,s}^\dagger \sigma^- + h.c.), \quad (58)$$

where the dispersion relation of photon is $\varepsilon_k^{(s)} = \omega_0^{(s)} - 2J_s \cos k$.

In the high energy limits $k \rightarrow \pm\pi/2$ and $\omega_0^{(s)} = \pi J_s$, the dispersion relation of the photon is $\varepsilon_k^{(s)} \sim v_s |k|$ with the group velocity $v_s = 2J_s$. In the case, the Hamiltonian (58) describes the photon transport in the H-type waveguide. For convenient, we use the operators

$$a_{k,e}^{(s)} = \frac{1}{\sqrt{2}} (a_{k,s} + a_{-k,s}),$$

$$a_{k,o}^{(s)} = \frac{1}{\sqrt{2}} (a_{k,s} - a_{-k,s}), \quad (59)$$

to rewrite the Hamiltonian (58) as $H_H = H_H^{(e)} + H_H^{(o)}$, where

$$H_H^{(o)} = \sum_{k>0,s=1,2} \varepsilon_k^{(s)} a_{k,o}^{(s)\dagger} a_{k,o}^{(s)}, \quad (60)$$

for the o -photon and

$$H_H^{(e)} = \Omega |e\rangle \langle e| + \sum_{k>0,s=1,2} \varepsilon_k^{(s)} a_{k,e}^{(s)\dagger} a_{k,e}^{(s)}$$

$$+ \frac{1}{\sqrt{L}} \sum_{k>0,s=1,2} (\bar{V}_s a_{k,e}^{(s)\dagger} \sigma^- + h.c.), \quad (61)$$

for the e -photon with the effective coupling $\bar{V}_s = \sqrt{2}V_s$. Because Hamiltonian $H_H^{(o)}$ is diagonalized in the bases $\{a_{k,o}^{(s)\dagger} |0\rangle\}$, so we only need to find the S -matrix for the e -photon.

A. The LSZ reduction for e -photon scattering in the H-type waveguide

For calculating the multi-photon S -matrix, we only consider the Green's function and the S -matrix for the e -photon in the H-type waveguide. In this case, the $2n$ -point photonic Green's function reads

$$G_{p_1, \dots, p_n; k_1, \dots, k_n}^{j_1, \dots, j_n; i_1, \dots, i_n}(t'_1, \dots, t'_n; t_1, \dots, t_n) \quad (62)$$

$$= \left\langle T a_{p_1, e}^{(j_1)}(t'_1) \dots a_{p_n, e}^{(j_n)}(t'_n) a_{k_1, e}^{(i_1)\dagger}(t_1) \dots a_{k_n, e}^{(i_n)\dagger}(t_n) \right\rangle_H.$$

The S -matrix element is the overlap

$$out \langle f | i \rangle_{in} = in \langle f | S | i \rangle_{in}, \quad (63)$$

of incoming wave $|i\rangle_{in} = a_{k_1, e}^{(i_1)\dagger} \dots a_{k_n, e}^{(i_n)\dagger} |0\rangle$ and outgoing wave state $|f\rangle_{out}$. As shown in the Sec. III, the basic part of the S -matrix is the T -matrix. The relation

$$iT_{2n}^{(H)} = G_{2n}^{(H)} \prod_{r=1}^n [2\pi G_{0i_r}^{-1}(k_r) G_{0j_r}^{-1}(p_r)] \Big|_{os}, \quad (64)$$

between the $2n$ -point T -matrix element

$$T_{2n}^{(H)} = T_{p_1, \dots, p_n; k_1, \dots, k_n}^{j_1, \dots, j_n; i_1, \dots, i_n}, \quad (65)$$

and the $2n$ -point Green's function

$$G_{2n}^{(H)} = G_{p_1, \dots, p_n; k_1, \dots, k_n}^{j_1, \dots, j_n; i_1, \dots, i_n}, \quad (66)$$

is determined by the LSZ reduction approach, where

$$G_{0i_r}(k_r) = \frac{i}{\omega_r - \varepsilon_{k_r}^{(i_r)} + i0^+}, \quad (67)$$

is the Green's function of the free photon and $G_{p_1, \dots, p_n; k_1, \dots, k_n}^{j_1, \dots, j_n; i_1, \dots, i_n}$ is the Fourier transformation of Eq. (62). Here, the subscript *os* denotes the on shell limits $\omega \rightarrow \varepsilon_k^{(i)}$. Then, the $2n$ -point Green's function

$$G_{p_1, \dots, p_n; k_1, \dots, k_n}^{j_1, \dots, j_n; i_1, \dots, i_n} = \frac{(-1)^n \delta^{2n} \ln Z[\eta_k^s, \eta_k^{s*}]}{\delta \eta_{p_1}^{j_1*} \dots \delta \eta_{p_n}^{j_n*} \delta \eta_{k_1}^{i_1} \dots \delta \eta_{k_n}^{i_n}} \Bigg|_{\eta_k^s = \eta_k^{s*} = 0}, \quad (68)$$

is obtained by the generating functional

$$\ln Z[\eta_k^s, \eta_k^{s*}] = Tr \ln M[\xi, \xi^*] - i \sum_s \int d\omega dk \frac{|\eta_k^s(\omega)|^2}{\omega - \varepsilon_k^{(s)} + i0^+}, \quad (69)$$

where we have used the matrix

$$M[\xi, \xi^*] = \begin{pmatrix} [\omega - \Omega + i\Gamma_e/2] \delta_{\omega\omega'} & \xi(\omega - \omega') \\ \xi^\dagger(\omega' - \omega) & (\omega - i0^+) \delta_{\omega\omega'} \end{pmatrix}, \quad (70)$$

and the field variable

$$\xi(\omega) = \sum_s \int \frac{dk}{2\pi} \frac{\bar{V}_s \eta_k^s(\omega)}{\omega - \varepsilon_k^{(s)} + i0^+}. \quad (71)$$

Here, the atom decay rate is $\Gamma_e = \sum_s \bar{V}_s^2 / v_s$. Finally, together with Eqs. (68) and (69), Eq. (64) gives the basic element of the S -matrix, i.e., T -matrix. Using the T -matrix elements, we can find the all S -matrix elements. For convenient, we let $v_1 = v_2 = 1$ below.

B. Single and two e -photon S -matrices

We consider the single and the two e -photon S -matrices in this subsection. The diagrammatic analysis shows that the single e -photon S -matrix element

$$S_{p;k}^{j;i} = \delta_{kp} \delta_{ij} + iT_{p;k}^{j;i}, \quad (72)$$

consists of the T -matrix element

$$iT_{p;k}^{j;i} = G_{p;k}^{j;i} [2\pi G_{0j}^{-1}(p) G_{0i}^{-1}(k)] \Big|_{os}, \quad (73)$$

where k and p are the momenta of the incoming photon in the waveguide- i and the outgoing photon in the waveguide- j respectively. Together with Eq. (68) and Eq. (69), we obtain the single e -photon T -matrix element as

$$iT_{p;k}^{j;i} = \frac{-i\bar{V}_i \bar{V}_j}{k - \Omega + i\frac{1}{2}\Gamma_e} \delta_{kp}. \quad (74)$$

Next, we consider the special case: the incident e -photon is prepared in the waveguide-1. Then, the S -matrix elements are $S_{p;k}^{1;1} = t_k^{(11)} \delta_{kp}$ and $S_{p;k}^{2;1} = t_k^{(21)} \delta_{kp}$, for

$$t_k^{(11)} = \frac{k - \Omega + i\frac{1}{2}(\bar{V}_2^2 - \bar{V}_1^2)}{k - \Omega + i\frac{1}{2}(\bar{V}_2^2 + \bar{V}_1^2)}, \quad (75)$$

and

$$t_k^{(21)} = \frac{-i\bar{V}_1 \bar{V}_2}{k - \Omega + i\frac{1}{2}\Gamma_e}. \quad (76)$$

We can verify the unitarity of the S -matrix as

$$|t_k^{(11)}|^2 + |t_k^{(21)}|^2 = 1. \quad (77)$$

For the two photon case, the diagrammatic analysis and the LSZ reduction approach give the two e -photon S -matrix element

$$S_{p_1 p_2; k_1 k_2}^{j_1 j_2; i_1 i_2} = S_{p_1 k_1}^{j_1 i_1} S_{p_2 k_2}^{j_2 i_2} + S_{p_2 k_1}^{j_2 i_1} S_{p_1 k_2}^{j_1 i_2} + iT_{p_1 p_2; k_1 k_2}^{j_1 j_2; i_1 i_2}, \quad (78)$$

with the two photon T -matrix element

$$iT_{p_1 p_2; k_1 k_2}^{j_1 j_2; i_1 i_2} = G_{p_1 p_2; k_1 k_2}^{j_1 j_2; i_1 i_2} \prod_{r=1}^2 [2\pi G_{0i_r}^{-1}(k_r) G_{0j_r}^{-1}(p_r)] \Big|_{os}, \quad (79)$$

where k_r and p_r are the momenta of the incoming photons in the waveguide- i_r and the outgoing photons in the waveguide- j_r respectively. Together with Eqs. (68) and (69), the two e -photon T -matrix element becomes

$$iT_{p_1 p_2; k_1 k_2}^{j_1 j_2; i_1 i_2} = \frac{i\bar{V}_{i_1} \bar{V}_{i_2} \bar{V}_{j_1} \bar{V}_{j_2} (k_1 + k_2 - 2\alpha_H)}{\pi(p_2 - \alpha_H)(k_1 - \alpha_H)} \times \frac{\delta_{k_1+k_2, p_1+p_2}}{(p_1 - \alpha_H)(k_2 - \alpha_H)}, \quad (80)$$

with $\alpha_H = \Omega - i\Gamma_e/2$.

Finally, we consider the special case: the two incident e -photons are prepared in the waveguide-1 and the waveguide-2 respectively, i.e., the incident state $|in\rangle$ is $|in\rangle = a_{k_1, e}^{(1)\dagger} a_{k_2, e}^{(2)\dagger} |0\rangle$. In this case, Eqs. (78) and (80) give the S -matrix elements as

$$S_{p_1 p_2; k_1 k_2}^{1,1; 1,2} = t_{k_1}^{(11)} t_{k_2}^{(21)} (\delta_{k_1 p_1} \delta_{k_2 p_2} + \delta_{k_1 p_2} \delta_{k_2 p_1}) + \frac{i\bar{V}_2 \bar{V}_1^3}{\pi} \frac{(k_1 + k_2 - 2\alpha_H)}{(p_2 - \alpha_H)(k_1 - \alpha_H)} \times \frac{\delta_{k_1+k_2, p_1+p_2}}{(p_1 - \alpha_H)(k_2 - \alpha_H)}, \quad (81)$$

$$S_{p_1 p_2; k_1 k_2}^{1,2; 1,2} = t_{k_1}^{(11)} t_{k_2}^{(22)} \delta_{k_1 p_1} \delta_{k_2 p_2} + t_{k_1}^{(21)} t_{k_2}^{(21)} \delta_{k_1 p_2} \delta_{k_2 p_1} + \frac{i\bar{V}_1^2 \bar{V}_2^2}{\pi} \frac{(k_1 + k_2 - 2\alpha_H)}{(p_2 - \alpha_H)(k_1 - \alpha_H)} \times \frac{\delta_{k_1+k_2, p_1+p_2}}{(p_1 - \alpha_H)(k_2 - \alpha_H)}, \quad (82)$$

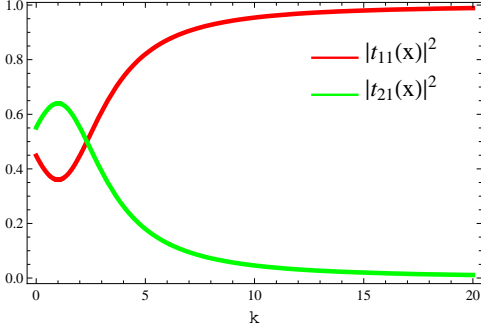


FIG. 11: (Color online) The transmission coefficients in the waveguide-1 and the waveguide-2: $\bar{V}_1 = 1$, $\bar{V}_2 = 2$. The energy level spacing Ω is taken as the unit.

and

$$S_{p_1 p_2; k_1 k_2}^{2,2;1,2} = t_{k_1}^{(21)} t_{k_2}^{(22)} (\delta_{k_1 p_1} \delta_{k_2 p_2} + \delta_{k_1 p_2} \delta_{k_2 p_1}) + \frac{i \bar{V}_1 \bar{V}_2^3}{\pi} \frac{(k_1 + k_2 - 2\alpha_H)}{(p_2 - \alpha_H)(k_1 - \alpha_H)} \times \frac{\delta_{k_1 + k_2, p_1 + p_2}}{(p_1 - \alpha_H)(k_2 - \alpha_H)}. \quad (83)$$

Here, $t_k^{(22)}$ is defined by

$$t_k^{(22)} = \frac{k - \Omega + i\frac{1}{2}(\bar{V}_1^2 - \bar{V}_2^2)}{k - \Omega + i\frac{1}{2}(\bar{V}_1^2 + \bar{V}_2^2)}. \quad (84)$$

C. The state of the outgoing photons

With the help of the S -matrix elements obtained in the above subsection, we find that for the single incident e -photon prepared in the waveguide-1, the out-state of the scattered photon is

$$|out\rangle = (t_k^{(11)} a_{k,e}^{(1)\dagger} + t_k^{(21)} a_{k,e}^{(2)\dagger}) |0\rangle. \quad (85)$$

As the functions of the incident momentum k , the $t_k^{(11)}$ and $t_k^{(21)}$ are plotted in Fig. 11. We find that if $\bar{V}_2^2 = \bar{V}_1^2$, the transmission coefficient $t_k^{(11)}$ equals to zero when $k = \Omega$ (Fig. 12). This result displays that the outgoing e -photon is only emitted from the waveguide-2 when the incident e -photon is on resonance with the atom.

For the case of the two incident e -photons prepared in the different waveguides, i.e., the state $|in\rangle$ of the incident photons is

$$|in\rangle = a_{k_1,e}^{(1)\dagger} a_{k_2,e}^{(2)\dagger} |0\rangle. \quad (86)$$

From Eqs. (81-83), we obtain the out-state of the scattered photons as

$$|out\rangle = |out\rangle_{11} + |out\rangle_{12} + |out\rangle_{22}, \quad (87)$$

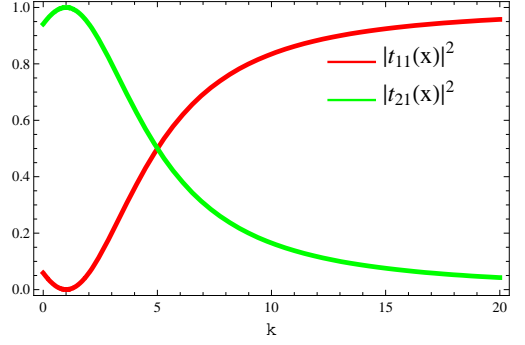


FIG. 12: (Color online) The transmission coefficients in the waveguide-1 and the waveguide-2: $\bar{V}_1 = \bar{V}_2 = 2$. The energy level spacing Ω of the atom is taken as the unit. If the incident photon is on resonance with the atom, the transmission coefficient in the waveguide-1 equals zero and that in the waveguide-2 equals one. this result displays that the outgoing photon only emits from waveguide-2.

with three parts: (a) the state of the two outgoing e -photons both in the waveguide-1 is

$$|out\rangle_{11} = \sum_{p_1 \leq p_2} S_{p_1 p_2; k_1 k_2}^{1,1;1,2} a_{p_1,e}^{(1)\dagger} a_{p_2,e}^{(1)\dagger} |0\rangle; \quad (88)$$

(b) the state of the two outgoing e -photons in the different waveguides is

$$|out\rangle_{12} = \sum_{p_1, p_2} S_{p_1 p_2; k_1 k_2}^{1,2;1,2} a_{p_1,e}^{(1)\dagger} a_{p_2,e}^{(2)\dagger} |0\rangle; \quad (89)$$

(c) the state of the two outgoing e -photons both in the waveguide-2 is

$$|out\rangle_{22} = \sum_{p_1 \leq p_2} S_{p_1 p_2; k_1 k_2}^{2,2;1,2} a_{p_1,e}^{(2)\dagger} a_{p_2,e}^{(2)\dagger} |0\rangle. \quad (90)$$

In the spatial representation, the state of the outgoing e -photon

$$|out\rangle = \int dx_1 dx_2 e^{iEx_c} [g_{11}(x_c, x) a_{x_1,e}^{(1)\dagger} a_{x_2,e}^{(1)\dagger} + g_{12}(x_c, x) a_{x_1,e}^{(1)\dagger} a_{x_2,e}^{(2)\dagger} + g_{22}(x_c, x) a_{x_1,e}^{(2)\dagger} a_{x_2,e}^{(2)\dagger}] |0\rangle, \quad (91)$$

is determined by the wavefunction in the center of mass frame $x_c = (x_1 + x_2)/2$ with the relative coordinate $x = x_1 - x_2$: (a) the wavefunction $g_{11}(x)$ of two photons both in the waveguide-1 is obtained as

$$g_{11}(x) = \frac{1}{2\pi} [t_{k_1}^{(11)} t_{k_2}^{(21)} \cos(\Delta_k x) - \frac{4\bar{V}_2 \bar{V}_1^3 e^{i(E/2 - \alpha_H)|x|}}{4\Delta_k^2 - (E - 2\alpha_H)^2}]; \quad (92)$$

(b) the wavefunction $g_{12}(x)$ of two photons in the different waveguides is obtained as

$$g_{12}(x) = \frac{1}{2\pi} [(t_{k_1}^{(11)} t_{k_2}^{(22)} + t_{k_1}^{(21)} t_{k_2}^{(21)}) \cos(\Delta_k x) + i(t_{k_1}^{(11)} t_{k_2}^{(22)} - t_{k_1}^{(21)} t_{k_2}^{(21)}) \sin(\Delta_k x) - \frac{8\bar{V}_1^2 \bar{V}_2^2 e^{i(E/2 - \alpha_H)|x|}}{4\Delta_k^2 - (E - 2\alpha_H)^2}]; \quad (93)$$

(c) the wavefunction $g_{22}(x)$ of the two photons both in the waveguide-2 is obtained as

$$g_{22}(x) = \frac{1}{2\pi} [t_{k_1}^{(21)} t_{k_2}^{(22)} \cos(\Delta_k x) - \frac{4\bar{V}_1 \bar{V}_2^3 e^{i(E/2 - \alpha_H)|x|}}{4\Delta_k^2 - (E - 2\alpha_H)^2}], \quad (94)$$

where we define $E = k_2 + k_1$ and $\Delta_k = (k_1 - k_2)/2$.

D. Quantum statistics by second order correlation functions

Finally, we analyze the quantum statistical features of the scattered photon by the second order correlation functions of photons. The second order correlation function of the outgoing e -photon is defined by

$$G_{ij}^{(2)}(x_1, x_2) = \langle out | a_{x_1, e}^{(i)\dagger} a_{x_2, e}^{(j)\dagger} a_{x_2, e}^{(j)} a_{x_1, e}^{(i)} | out \rangle. \quad (95)$$

It is straightforward to prove that the second order correlation is just $|g_{ij}(x)|^2$ by substituting Eq. (91) into Eq. (95). Thus the wavefunction $g_{ij}(x)$ displays the quantum statistic characters of the scattered photons. Here, the second order correlation function $|g_{ij}(x)|^2$ are plotted in Fig. 13 and Fig. 14 for different system parameters. In these figures, we take the energy level spacing of the atom as unit and the total energy of the incident two e -photons equal to two, i.e., two times of the energy level spacing of the atom.

Fig. 13 shows that if $\bar{V}_1 = \bar{V}_2 = 2$, the outgoing two e -photons attract with each other through the interaction with the atom. This displays the obvious bunching behavior of photons. In Fig. 13a, the two incident photons are both on resonance with the atom, so $|g_{11}(x)|^2 = |g_{22}(x)|^2$. Fig. 14 shows that when $\bar{V}_1 \neq \bar{V}_2$, such as $\bar{V}_1 = 1$ and $\bar{V}_2 = 2$, if the outgoing two e -photons are emitted from the same waveguide they attract with each other and display the photon bunching behavior. If the outgoing two e -photons are emitted from the different waveguides, they display the photon bunching behavior when the two photons are both on resonance with the atom.

By adjusting the difference $\Delta V = \bar{V}_2 - \bar{V}_1$ between the interactions \bar{V}_1 and \bar{V}_2 , we find that (a) If the two photons are both resonance with the atom, the out-going photons always display the photon bunching behavior, however, when ΔV increases the photon bunching behavior becomes vague and in the limit $\Delta V \rightarrow \infty$, $|g_{11}(x)|^2$,

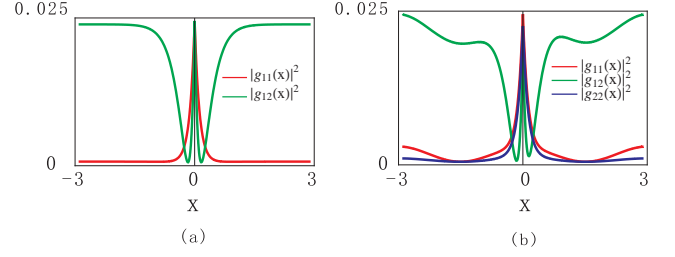


FIG. 13: (Color online) The correlations of the two photons in the center of mass frame: $\bar{V}_1 = \bar{V}_2 = 2$. The energy level spacing Ω of the atom is taken as the unit. (a) The total energy of the incident photons E is 2, and the difference Δ_k of two incident energies is zero. In this case, the two photons are both on resonance at the atom. (b) The total energy of the incident photons E is 2, and the difference Δ_k of two incident energies is 1.

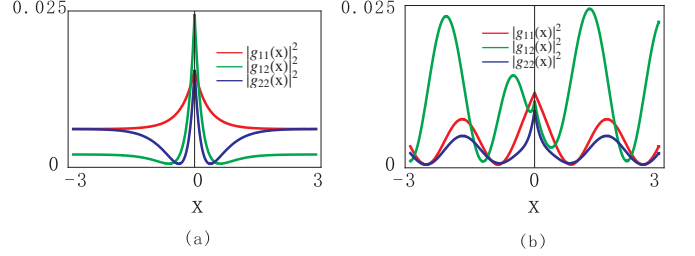


FIG. 14: (Color online) The correlations of the two photons in the center of mass frame: $\bar{V}_1 = 1$ and $\bar{V}_2 = 2$. The energy level spacing Ω of the atom is taken as the unit. (a) The total energy of the incident photons E is 2, and the difference Δ_k of two incident energies is zero. In this case, the two photons are both on resonance on the atom. (b) The total energy of the incident photons E is 2, and the difference Δ_k of two incident energies is 1.8.

$|g_{22}(x)|^2$ and $|g_{12}(x)|^2$ all tend to constants which implies the photon bunching behavior disappears. (b) If the two photons are not resonance with the atom and the total energy equals to 2Ω , the functions $|g_{11}(x)|^2$, $|g_{22}(x)|^2$ and $|g_{12}(x)|^2$ exhibit the oscillation behaviors. As $\Delta V \rightarrow \infty$, $|g_{11}(x)|^2$, $|g_{22}(x)|^2$ and $|g_{12}(x)|^2$ all tend to constants and the oscillation behavior disappears.

To summarize this section, we have used the LSZ reduction approach to investigate the single photon transmission and the quantum statistic properties of the two photon transport in the H-type waveguide. The transport of multi-photon in the more complex CRA can be investigated systematically by the same method.

VII. SUMMARY

In conclusion, we have demonstrated that the LSZ approach is feasible to be generalized for studying the complex nano-structure for multi-photon transport, such

as the multi-photon transport problems in the complex CRA systems. Concretely, the single-, two- and three-photon transports in the T-type waveguide are investigated by the LSZ approach in details. Some of our results accord with the known results obtained by other methods for the simple case. Besides, the scattering of three photons in the T-type waveguide and the quantum statistical characters of two photons in the H-type waveguide are systematically studied by this approach. For the single photon transmission in the T-type CRA, we find two bound states: the lower bound state is below the bottom of the photon energy band, the upper bound state is above the top of the photon energy band. We also gives the three-photon scattering wave function by the LSZ approach. Obviously, the LSZ reduction approach can be carried out to investigate the N -photon transport in the more complex architectures constructed by the T-type CRA.

Finally, we emphasize that the LSZ reduction approach can be extended to investigate not only the multi-photon scattering problem in the quantum optics, but also the scattering processes in other fields, such as the Kondo scattering in the condensed matter physics and the Feshbach resonance^{19,39} in the atomic physics. It is more interesting to simulate the scattering processes in the condensed matter physics or the atomic physics by the complex CRA architectures. By making use of the LSZ reduction approach, we can study the photon scattering in these artificial CRA architectures to understand the realistic scattering processes as well as electron transport⁴⁰⁻⁴² in the condensed matter physics.

Acknowledgments

This work is supported by NSFC No. 10474104, No. 60433050, and No. 10704023, NFR-PCNo. 2006CB921205 and 2005CB724508.

Appendix: Multi-photon eigenstates in the T-type CRA

In the appendix, we utilize the scattering Bethe ansatz^{37,38} to obtain the multi-photon eigenstates. For convenient, we start with the Hamiltonian (41). In the real space, the Hamiltonian (41) is rewritten as $H_T^e = H_p + H_a + H_{int}$, where the Hamiltonian of photons is

$$H_p = -i \int dx \psi^\dagger(x) \partial_x \psi(x), \quad (\text{A.1})$$

and the Hamiltonian of two-level atom is $H_a = \Omega |e\rangle \langle e|$. The interaction Hamiltonian H_{int} is

$$H_{int} = \bar{V} \int dx \delta(x) (\psi(x) \sigma^+ + h.c.). \quad (\text{A.2})$$

Here,

$$\psi(x) = \frac{1}{\sqrt{L}} \sum_k a_{k,e} e^{ikx}, \quad (\text{A.3})$$

is the Fourier transformation of $a_{k,e}$. The single photon eigenstates are constructed by

$$|\phi_p\rangle = \left[\int dx f_p(x) \psi^\dagger(x) + e_p \sigma^+ \right] |0\rangle. \quad (\text{A.4})$$

The Schrodinger equation $H_T^e |\phi_p\rangle = p |\phi_p\rangle$ gives

$$|p\rangle = \int dx e^{ipx} \alpha_p^\dagger(x) |0\rangle. \quad (\text{A.5})$$

where we define an operator

$$\alpha_p^\dagger(x) = [\theta(-x) + e^{i\delta_p} \theta(x)] \psi^\dagger(x) + \delta(x) e_p \sigma^+, \quad (\text{A.6})$$

which is the single photon creation operator $\psi^\dagger(x)$ when \bar{V} tends to zero. However, when \bar{V} is not zero, $\alpha_p^\dagger(x)$ neither satisfies the bosonic commutation relation nor the fermionic commutation relation. Here, e_p and $f_p(x)$ are

$$e_p = \frac{V}{p - \Omega + i\Gamma/2}, \quad (\text{A.7})$$

$$f_p(x) = e^{ipx} [\theta(-x) + e^{i\delta_p} \theta(x)], \quad (\text{A.8})$$

where $\Gamma = \bar{V}^2$ and the phase shift

$$e^{i\delta_p} = \frac{p - \Omega - i\Gamma/2}{p - \Omega + i\Gamma/2}, \quad (\text{A.9})$$

is the same as t_k (45).

For studying the multi-photon eigenstates, we use the scattering Bethe-ansatz to assume the N -photon eigenstate

$$|\Phi\rangle_N = \sum_P A_P \int [Dx] e^{i \sum_j k_{P_j} x_j} \prod_{i=1}^N \alpha_{k_{P_i}}^\dagger(x_i) |0\rangle. \quad (\text{A.10})$$

Here, $[Dx]$ denotes $\prod_{i=1}^N \theta(x_{i+1} - x_i) dx_i$ and $P = (P_1, P_2, \dots, P_N)$ is a permutation of $(1, 2, \dots, N)$. The Schrodinger equation gives the relation $A_P/A_{P'} = e^{i\Phi(P_j, P_{j+1})}$, where the phase shift is

$$e^{i\Phi(P_j, P_{j+1})} = \frac{k_{P_j} - k_{P_{j+1}} - i\Gamma}{k_{P_j} - k_{P_{j+1}} + i\Gamma}, \quad (\text{A.11})$$

where $P = (P_1, P_2, \dots, P_j, P_{j+1}, \dots, P_N)$ and $P' = (P_1, P_2, \dots, P_{j+1}, P_j, \dots, P_N)$. As an example, we give the explicit expression of the three photon eigenstate

$$\begin{aligned} |\Phi\rangle_{N=3} &= \int \theta(x_3 - x_2) \theta(x_2 - x_1) \prod_i dx_i \\ & [1 + S_{12} + S_{23} + S_{12} S_{13} \\ & + S_{23} S_{13} + S_{12} S_{13} S_{23}] e^{ik_1 x_1 + ik_2 x_2 + ik_3 x_3} \\ & \times \alpha_{k_1}^\dagger(x_1) \alpha_{k_2}^\dagger(x_2) \alpha_{k_3}^\dagger(x_3) |0\rangle, \end{aligned} \quad (\text{A.12})$$

where

$$S_{ij} = \frac{k_j - k_i - i\Gamma}{k_j - k_i + i\Gamma} P_{ij}, \quad (\text{A.13})$$

and $P_{ij} f(\dots, k_i, \dots, k_j, \dots) = f(\dots, k_j, \dots, k_i, \dots)$. Here, f is any given function.

-
- ¹ D. E. Chang, A. S. Sørensen, E. A. Demler, and M. D. Lukin, Nat. Phys. **3**, 807 (2007).
² J. T. Shen and S. Fan, Phys. Rev. Lett. **95**, 213001 (2005).
³ C. P. Sun, L. F. Wei, Yu-xi Liu, and F. Nori, Phys. Rev. A **73**, 022318 (2006).
⁴ L. Zhou, Z. R. Gong, Y. X. Liu, C. P. Sun and F. Nori, Phys. Rev. Lett. **101**, 100501 (2008).
⁵ T. Shi, Y. Li, Z. Song, and C. P. Sun, Phys. Rev. A **71**, 032309 (2005).
⁶ S. Yang, Z. Song, and C. P. Sun, Phys. Rev. B **73**, 195122 (2006).
⁷ S. Yang, Z. Song, and C. P. Sun, Front. Phys. China **2**, 1 (2007).
⁸ J. T. Shen and S. Fan, Phys. Rev. Lett. **98**, 153003 (2007).
⁹ J. T. Shen and S. Fan, Phys. Rev. A **76**, 062709 (2007).
¹⁰ J. T. Shen and S. Fan, Opt. Lett. **30**, 2001 (2005).
¹¹ L. Zhou, J. Lu, and C. P. Sun, Phys. Rev. A **76**, 012313 (2007).
¹² F. M. Hu, L. Zhou, T. Shi, and C. P. Sun, Phys. Rev. A **76**, 013819 (2007).
¹³ A. L. Rakhmanov, A. M. Zagoskin, S. Savel'ev, and F. Nori, Phys. Rev. B **77**, 144507 (2008).
¹⁴ R. H. Dicke, Phys. Rev. **93**, 99 (1954).
¹⁵ K. Y. Bliokh, Y. P. Bliokh, V. Freilikher, S. Savel'ev, and F. Nori, Rev. Mod. Phys. **80**, 1201 (2008).
¹⁶ U. Fano, Phys. Rev. **124**, 1866 (1961).
¹⁷ P. W. Anderson, Phys. Rev. **124**, 41 (1961).
¹⁸ T. D. Lee, Phys. Rev. **95**, 1329 (1954).
¹⁹ D. Z. Xu, H. Ian, T. Shi, H. Dong, and C. P. Sun, arXiv: quant-ph/0812.0429.
²⁰ L. D. Landau and E. M. Lifshitz, *Quantum Mechanics (Nonrelativistic Theory)* (Butterworth, Boston 1991).
²¹ H. A. Bethe, Z. Physik **71**, 205 (1931).
²² C. N. Yang, Phys. Rev. Lett. **19**, 1312 (1967).
²³ M. T. Batchelor, Phys. Today **60**, 36 (2007).
²⁴ N. Andrei, Phys. Rev. Lett. **45**, 379 (1980).
²⁵ P. B. Wiegmann, JETP Lett. **31**, 364 (1980).
²⁶ P. B. Wiegmann, J. Phys. C **14**, 1463 (1981).
²⁷ P. B. Wiegmann and A. M. Tselick, J. Phys. C **16**, 2281 (1983).
²⁸ H. Lehmann, K. Symanzik, and W. Zimmermann, Nuovo Cimento **1**, 1425 (1955).
²⁹ G. Zarand, L. Borda, J. Delft, and N. Andrei, Phys. Rev. Lett. **93**, 107204 (2004).
³⁰ L. Borda, L. Fritz, N. Andrei, and G. Zarand, Phys. Rev. B **75**, 235112 (2007).
³¹ G. Källén and W. Pauli, Dan., Mat. Fys. Medd. **30**, 7 (1955).
³² T. D. Lee and G. C. Wick, Nucl. Phys. B **10**, 1 (1969).
³³ M. S. Maxon and R. B. Curtis, Phys. Rev. **137**, B996 (1965).
³⁴ M. S. Maxon, Phys. Rev. **149**, 1273 (1966).
³⁵ J. J. Sakurai, *Modern Quantum Mechanics* (Addison-Wesley, Reading, MA, 1994).
³⁶ J. R. Taylor, *Scattering Theory: The Quantum Theory on Non-relativistic Collision* (Wiley, New York, 1972).
³⁷ P. Mehta and N. Andrei, Phys. Rev. Lett. **96**, 216802 (2006).
³⁸ P. Mehta and N. Andrei, arXiv:cond-mat/0702612.
³⁹ H. Feshbach, Ann. Phys. **5**, 357-390 (1958).
⁴⁰ T. K. Ng and P. A. Lee, Phys. Rev. Lett. **61**, 1768 (1988).
⁴¹ Y. Meir, N. S. Wingreen, and P. A. Lee, Phys. Rev. Lett. **70**, 2601 (1993).
⁴² R. M. Konik, H. Saleur, and A. Ludwig, Phys. Rev. B **66**, 125304 (2002).